Tribol Lett (2014) 55:371–379
DOI 10.1007/s11249-014-0361-9

ORIGINAL PAPER

Effect of the Abrasive Size on the Friction Effectiveness and Instability of Brake Friction Materials: A Case Study with Zircon

M. W. Shin · Y. H. Kim · H. Jang

Received: 4 February 2014 / Accepted: 10 June 2014 / Published online: 25 June 2014

Abstract The friction-induced vibration triggered at the sliding interface between the gray iron disk and brake friction material was studied by changing the size of the zircon particles in the friction material. The friction tests were performed using a reduced brake dynamometer and the friction characteristics of the friction materials containing zircon particles with sizes of 3, 50, and 100 μm were analyzed. Our results show that the properties of the sliding surface were strongly affected by the entrenchment of the abrasive particles in the friction layers during sliding. The friction effectiveness was inversely proportional to the size of the abrasive, while friction instability was pronounced when smaller zircon particles were used. The smaller zircon particles produced larger plateaus on the sliding surface with low contact stiffness. However, the contact plateaus with the low contact stiffness showed higher amplitudes of the friction oscillations, suggesting a surface with low stiffness also can produce high propensity of friction instability during sliding. Based on the friction stability diagram and surface properties, such as contact stiffness and surface roughness, it was suggested that the static coefficient of friction, which was changed as a function of dwell time, was crucial to understand the cause of friction-induced force oscillations and propensity of friction instability of brake friction materials.

Keywords Brake · Friction material · Stick–slip · Abrasives · Zircon · Vibration

M. W. Shin · Y. H. Kim · H. Jang (✉)
Department of Materials Science and Engineering, Korea University, 1, 5-ga, Anam-dong, Seongbuk-gu, Seoul 136-713, South Korea
e-mail: hojang@korea.ac.kr

1 Introduction

Friction instability produced at the sliding interface has been considered as an important trigger for brake-induced noise and vibrations. Much effort has been directed toward reducing friction-induced excitation during braking by controlling the tribological properties of the friction materials and to prevent the amplification of the friction oscillation by avoiding resonance with other structural components [1–3]. For several decades, the methodology to decrease the brake noise and vibration has relied on approaches based on two different perspectives. One approach is to compensate the vibration by controlling the shape and stiffness of the components or by modifying the transfer function [4]. The second approach is to reduce friction oscillation at the sliding interface by regulating the interfacial properties of the sliding surfaces [5–7]. Since the two approaches complement each other, both approaches have been applied for the development of noiseless brake systems. However, friction-induced noise and vibrations have never disappeared and this can partially be ascribed to the lack of a fundamental understanding of the noise triggering mechanism, which is known to be closely associated to the tribological characteristics of the friction material.

In general, the control of the friction characteristics, such as the friction effectiveness and wear resistance is mainly carried out by changing the ingredients in the friction materials, although the contribution from the gray iron disks cannot be neglected [8, 9]. Recent commercial brake friction materials have demonstrated excellent wear resistance and fade resistance through the optimization of the formulation [10]. On the other hand, the effect of the ingredients on the friction-induced noise and vibration is very limited. Among the various ingredients used in the

friction material, abrasives are known to be closely related to the friction-induced vibration, while they are normally used to control the friction level through abrasive action against a gray iron disk and to remove pyrolized friction films on the disk surface during brake applications [10, 11].

Various inorganic hard particles, such as zircon, silicon carbide, alumina, quartz, magnesia, and iron oxides have been used as abrasives in commercial brake friction materials and the selection of them has been determined by their hardness, size, shape, fracture toughness, and aggressiveness against brake disks [8, 10, 12]. The size of the abrasive particle in particular, is known to affect the friction level, wear resistance of both friction materials and the counter disks, and the noise propensity of a brake system. Therefore, the proper selection of the abrasives sizes is crucial and the particle sizes ranging from few microns to several hundred microns in diameter have been used in commercial friction materials.

Various friction characteristics related to the type, amount, and size of the abrasives have been studied [11–16]. Jang and Kim [13] studied the effect of the relative amount of zircon and a solid lubricant (Sb_2S_3) in the friction material to investigate their synergistic effects. They found that zircon particles increased the torque variation during brake stops, while the friction oscillation was more sensitive to the solid lubricant. The effects of the abrasive particles on the brake performance also have been reported by Ma et al. [15] and Matejka et al. [16], while these studies focused more on the friction effectiveness and wear resistance of the friction materials rather than the friction-induced vibrations. Cho et al. [11] investigated the effect of the size of zircon on the friction instability and wear resistance of the friction material. They found that the coarse zircon particles reduced the oscillation amplitude of the friction coefficient, while resulting in excessive disk wear. On the other hand, the fine zircon particles produced transient friction films, causing excessive friction material wear and pronounced friction oscillation. Lee et al. [14] studied the friction and wear of the friction materials containing zircon or quartz. They found that the friction level and wear resistance were strongly affected by the type and size of the abrasives, although the friction instability was not examined. Kim et al. [13] investigated the stick–slip at low velocity affected by the type of the abrasives. They found that the stick–slip amplitude was determined by the hardness and fracture toughness of the abrasives. However, the study to understand the cause for friction instability induced by the abrasives has been very limited, although understanding the mechanism of the triggering the periodic friction oscillations is very important to eliminate friction-induced noise and vibration during brake applications.

In this study, the friction characteristics of friction materials containing zircon particles of three different sizes were investigated to understand the cause of the occurrence of friction oscillations at the sliding interface. We focused on the surface properties of the friction material after the friction tests, which directly engaged in the triggering of the friction oscillations during braking.

2 Experiments

Industrial grade zircon particles, termed as ZR 3, ZR 50, and ZR 100, with different particle sizes were used to produce the friction material specimens used in this study. The morphology of the zircon particles used in this study is shown in the Fig. 1. The average size of zircon was 101.7 ± 25.8 μm for ZR 100, 49.2 ± 28.7 μm for ZR 50, and 2.7 ± 1.1 μm for ZR 3. The size distribution of the zircon particles was relatively broad, as shown in Fig. 2.

A simplified formulation containing five ingredients was used to produce the friction material specimens. The amount of zircon was set to 10 vol%, which was greater than the normal abrasive content used in commercial brake friction materials. Table 1 shows the composition of the friction material specimens tested in this study. The friction material specimens were manufactured by dry mixing, preforming, hot pressing, and post-curing [8]. The mixing was carried out for 5 min using a high speed mixer (Eirich, Germany). The mix was preformed at room temperature under 20 MPa for 1 min and hot pressed at 180 °C under 35 MPa for 10 min with intermittent gas releases. Post-curing was carried out for 6 h at 200 °C using a convection oven. The size of the friction material specimen to be tested in the reduced scale dynamometer was 45 mm × 18 mm × 6 mm. The total contact area of the friction materials with the gray iron disks was 16.2 cm^2.

A reduced scale brake dynamometer (MoinSys, Korea) with a rigid caliper was used to study the friction characteristics of the friction material. A schematic of the dynamometer used in this study is shown in Fig. 3. A typical gray cast iron disk with A-type graphite flakes was used as the counter disk. The size of the gray iron disk was 160 mm in diameter and 8 mm in thickness. Before measuring the coefficient of friction at low speeds, a burnishing procedure was carried out to ensure the uniform contact of the friction materials on the disk surface and to develop steady friction films. The details of the test procedure used in this study are listed in Table 2. The tests were carried out in an environmental chamber maintained at approximately 5.5–7.3 g/m^3 AH, which is equivalent to 32–40 % RH. The surface topography of the friction materials and the counter disks was examined after the sliding tests using a laser confocal microscope (Keyence, Japan). The stiffness of the friction material was measured using a universal testing machine (Instron, USA).

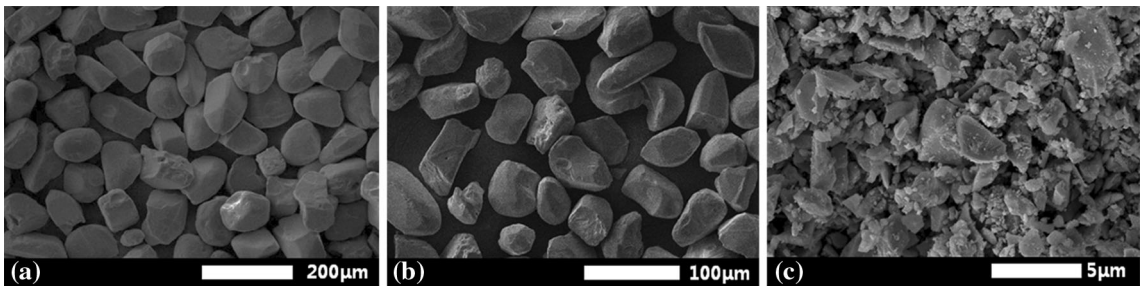

Fig. 1 Scanning electron microscopy (SEM) micrographs of the three different zircon particles used in this study. Average sizes of the particles were **a** 101.7 ± 25.8 μm for ZR 100, **b** 49.2 ± 28.7 μm for ZR 50, and **c** 2.7 ± 1.1 μm for ZR 3

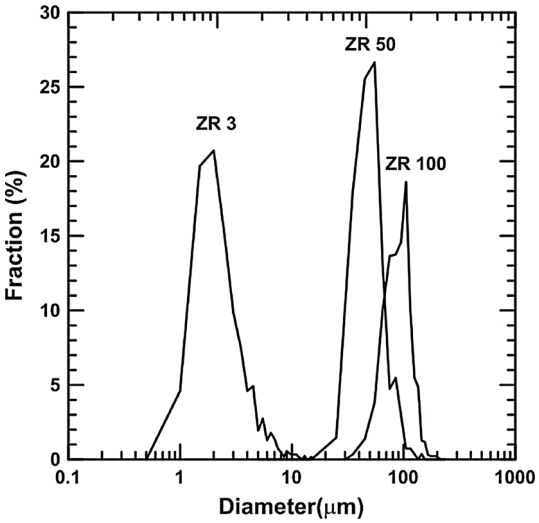

Fig. 2 Size distribution of the zircon particles used in this study. Commercially available zircon particles showed a broad size distribution

Table 1 Composition of the friction material investigated in this study

Classification	Ingredient	Vol%
Binder	Phenolic resin	15
Reinforcing fiber	Aramid fiber	10
Filler	Barite	55
Solid lubricant	Graphite	10
Abrasive	Zircon	10

3 Results and Discussion

3.1 Surface Morphology and Friction Effectiveness

The friction effectiveness of a braking system is determined by the complicated interaction at the sliding interface between the friction material and the gray iron disk. The molecular level interactions change the properties of the sliding interface, and hence, the surface after friction tests provides important information about the friction characteristics. In order to understand the effect of the zircon size on the friction characteristics, the correlation of the surface morphology and the friction level changed by the zircon size was examined first before analyzing the friction instability.

Figure 4 shows the average coefficient of friction of the friction material specimens with different zircon sizes. The average friction coefficient after the burnish procedure was higher when the fine zircon particles were used. Assuming that the zircon particles contribute to the formation of contact plateaus, the friction level appears to be determined by the total size of the contact area constructed by the zircon particles and the wear debris contacts accumulated around the hard particles [5]. A simple geometrical consideration supports the lower friction effectiveness resulting from large particles because the contact area occupied by the zircon particles decreases when the size of the zircon particles increases. This is consistent with the results reported by Lee et al. [14] in which high coefficient of friction and high wear rate were found in the case of using smaller zircon particles.

The change in the friction coefficient during the course of the burnish process was also examined since it is related to the formation of the friction film on the friction material surface during brake applications. The inset of Fig. 4 shows the traces of the friction coefficient up to the 100th stop during the burnish procedure, indicating steady state after more than 100 stops. This indicates that the friction material with fine zircon (ZR 3) reaches the steady friction level earlier than those with coarse zircon particles (ZR 50 and ZR 100).

The higher friction level and faster stabilization of the friction level with fine zircon particles are attributed to the large contact area produced by the smaller zircon particles and the fast formation of friction layer by compaction of wear debris around zircon particles. The faster saturation of the friction effectiveness with the fine zircon particles appears to provide a fast ramping rate of the brake torque during a stop. This is because the reconditioning of the friction material surface, including the redistribution of the

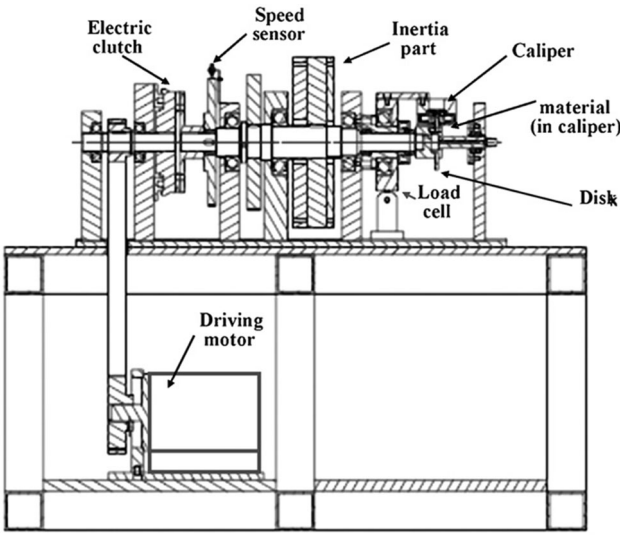

Fig. 3 The schematic of the reduced scale brake dynamometer

Table 2 Dynamometer test procedure carried out during the low speed test

Mode	Test condition
Burnish	Speed = 70 km/h, Pressure = 3 MPa
	Initial brake temperature = 120 °C
	Repeated 200 times in a constant pressure mode
Low speed drag	Drag velocity = 0.12–15.0 mm/s
	Line pressure = 1, 2, 4 MPa
	Initial brake temperature = 20–25 °C, Humidity = 5.5–7.3 g/m^3 AH (32–40 % RH)

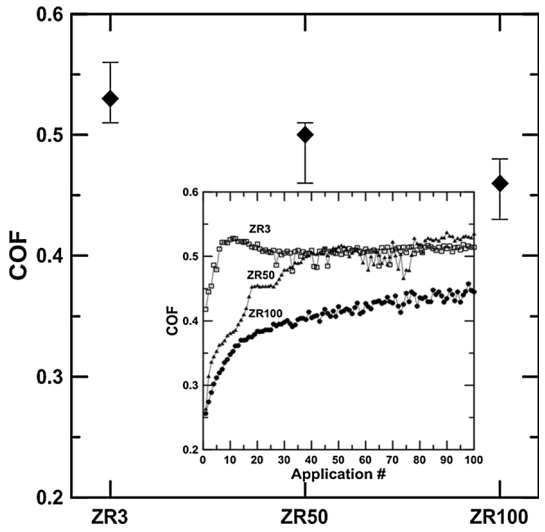

Fig. 4 The average friction coefficient of the friction materials with ZR3, ZR50, and ZR100 obtained after 200 burnish stops. The *inset* indicates the change in the friction coefficient during the burnish procedure up to the 100th burnish stop

ingredients and formation of a new friction film, occurs faster at the sliding interface with fine zircon particles [11]. The average wear rate of the friction materials, 0.41×10^{-3} mm^3/Nm, 0.96×10^{-3} mm^3/Nm, and 1.41×10^{-3} mm^3/Nm with ZR 100, ZR 50, and ZR 3, respectively, also support the easier formation of secondary plateaus when the smaller zircon particles are used. This is consistent with the results obtained in the case of other abrasive particles [13, 14].

The surface morphology of the burnished friction materials was examined after burnish to find the correlation with friction characteristics and shown in Fig. 5. The figure shows larger contact plateaus in the case of fine zircon (ZR3), while the surfaces with coarse zircon particles (ZR 100 and ZR 50) showed a few primary plateaus mainly by zircon particles. The worn surfaces indicate that the ingredients other than zircon are crushed or ground and do not play as a primary plateau. The surface roughness measured after the tests supports the larger contact area in the case of the fine zircon specimen (Table 3). The surface roughness parameters in the table support the micrographs in Fig. 5 showing that the coarse zircon particles (ZR 50 and ZR 100) were attached well to the matrix of the friction material, while the fine particles (ZR 3) were entrenched by the wear debris compacts and produced relatively uniform surface. The surface roughness of the gray iron disks after the tests were also examined, and the results are shown in Fig. 6 and Table 3. We examined the gray iron disk surfaces because they also affect the friction characteristics of the sliding interface [8, 9]. The results indicate that the disk surface tested with the friction material with fine zircon particles is more uniform compared to the disk surfaces rubbed with friction materials with coarse zircon. This is similar to the results obtained from a previous study by Lee et al. [14], indicating severe disk damage after testing with friction materials containing coarse zircon particles.

3.2 Friction-induced Force Oscillation

The brake-induced friction oscillation produced at the sliding interface has been considered to trigger brake noise and vibrations in a wide range of frequencies. In order to investigate the noise triggering mechanism and its relationship with the friction instability at the sliding interface, the shape of the torque oscillation was investigated in detail. Figure 7 shows the torque oscillation when the friction materials with ZR 3, ZR 50, and ZR 100 were slid at different sliding velocities at 4 MPa. The figure indicates that the torque amplitude and its frequency change from stick–slip to harmonic oscillation and is followed by smooth sliding with increase in the sliding velocity. The dependence of the stick–slip amplitude on the velocity was first proposed by Rabinowicz [17] and later by Gao et al. [18]. It was suggested that the amplitude of the stick–slip

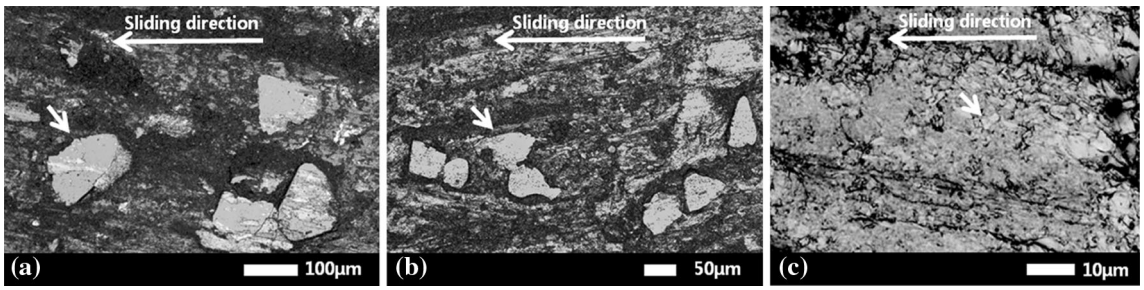

Fig. 5 Worn surfaces of the friction materials with **a** ZR 100, **b** ZR 50, and **c** ZR 3 after the burnish test. The zircon particles entrenched by wear debris compacts in the friction layers are indicated by *arrows*

Table 3 The surface roughness parameters obtained from an area of 30 mm × 10 mm using a laser confocal microscope

		R_a (μm)	R_p (μm)	S_m (μm)	σ (μm)
ZR 100	Friction material	4.18 ± 0.36	23.25 ± 5.4	254 ± 8.7	5.11
	Disk	1.56 ± 0.03	8.17 ± 0.39	227 ± 32.7	1.25
ZR 50	Friction material	3.78 ± 0.73	16.65 ± 3.8	296 ± 42.4	4.57
	Disk	1.38 ± 0.04	4.60 ± 0.41	123 ± 11.2	1.13
ZR 3	Friction material	2.15 ± 0.18	10.28 ± 2.1	263 ± 33.9	2.68
	Disk	0.87 ± 0.02	3.27 ± 0.15	51.47 ± 2.06	0.93

R_a: roughness average, R_p: maximum peak height, S_m: mean spacing of peaks, and σ: standard deviation of the asperity height distribution

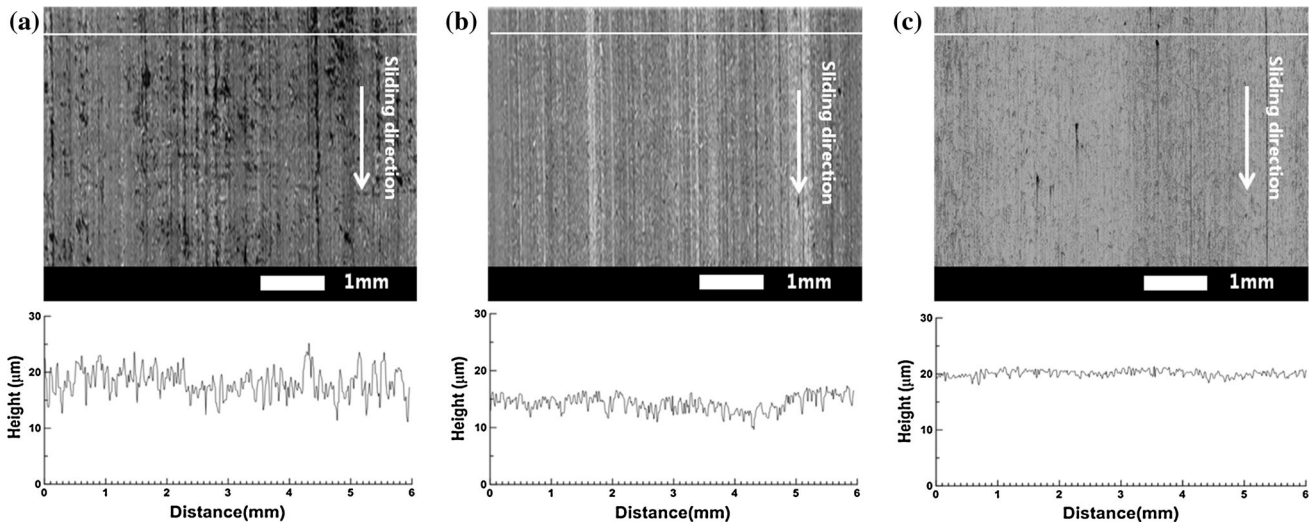

Fig. 6 Optical microscopy (OM) images and the surface profiles obtained from the worn surfaces of the counter disks tested with friction materials containing **a** ZR 100, **b** ZR 50, and **c** ZR 3

was proportional to L/kv, where k is the stiffness of the sliding system, v is the velocity, and L is the applied load, as the small torque amplitude seen at high sliding velocity in Fig. 7. The figure shows that the transition from stick–slip to smooth sliding is rather continuous and no abrupt transition was observed. The continuous decrease of the amplitude of friction oscillation is comparable to the case of sliding with lubricants with strong adsorbate–substrate interactions [19]. This is contrary to the results obtained by Fuadi et al. [20] who demonstrated a sharp transition from stick–slip to smooth sliding at the critical velocity.

Another salient feature of Fig. 7 is the fact that the friction characteristics, including the shape, amplitude, and frequency of torque oscillation, are also affected by the size of the zircon particles in the friction materials. At the same sliding velocity, the torque amplitude and the time of stick

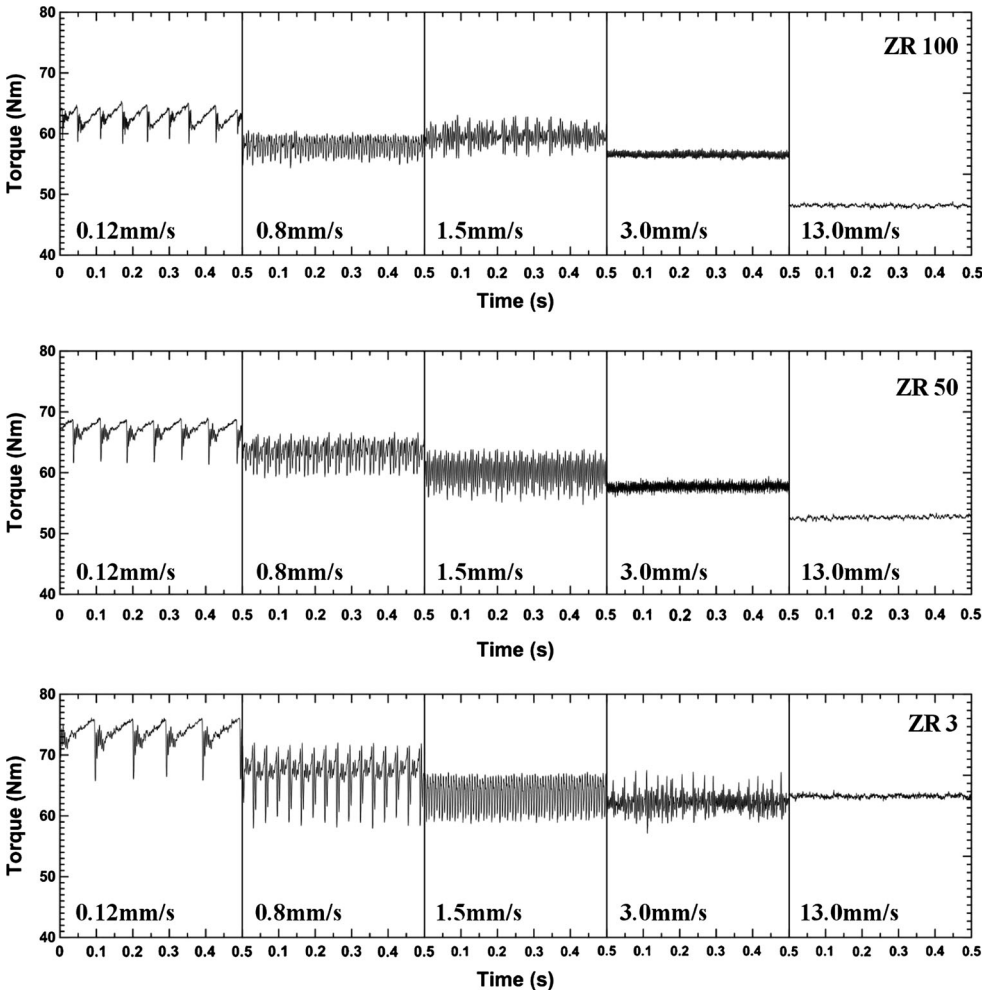

Fig. 7 Torque oscillations observed during sliding when friction material specimens with ZR 100, ZR 50, and ZR 3 were tested. The oscillation amplitude and critical velocity for smooth friction were affected by the size of zircon included in the friction material

period increased with decrease in the size of the zircon particles. The velocity dependent friction oscillation affected by the size of the zircon particles is represented as a function of the sliding velocity in Fig. 8. This plot shows that the amplitude of the torque oscillation decreases as a function of the sliding velocity and it decreases more rapidly when the size of zircon particles was larger, indicating that the torque oscillation is minimized at a lower critical velocity when coarse zircon particles are used in the friction material. Therefore, the disappearance of torque oscillation at a low critical velocity while using coarse zircon particles (ZR 100) indicates the low propensity of brake-induced friction instability. In order to find the domains of friction instability, the type of the torque oscillation was presented as a function of the pressure and velocity in a friction stability diagram (Fig. 9). The diagrams show that the friction oscillation appears up to higher critical velocity when the friction material contains fine zircon and the friction oscillation is pronounced at high pressure levels. The diagrams also show high-frequency

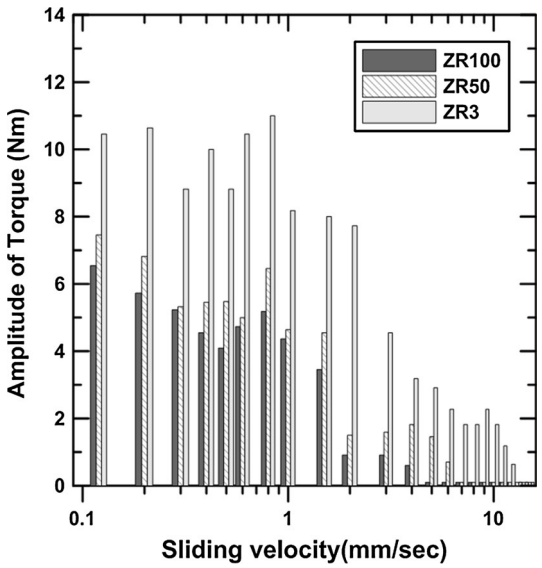

Fig. 8 Amplitude of the brake torque variation measured during sliding at 4 MPa as a function of the sliding velocity

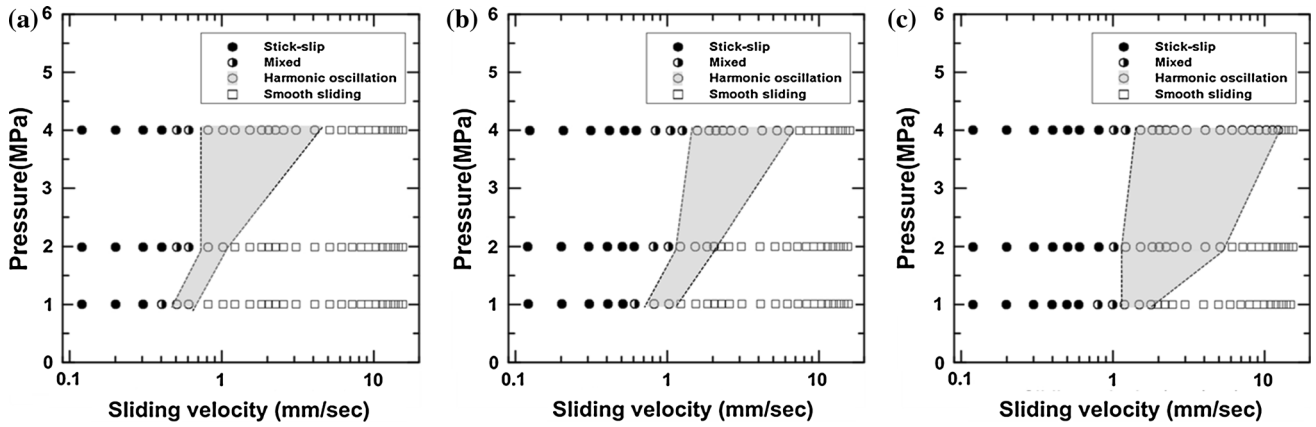

Fig. 9 Pressure–velocity diagrams showing the domains corresponding to stick slip, harmonic oscillation, and smooth sliding when friction tests were carried out using the friction materials with **a** ZR 100, **b** ZR 50, and **c** ZR 3

transient states, such as harmonic oscillations with nearly periodic features, between stick–slip and smooth sliding.

Similar results of ingredient effects have been observed in other studies on brake friction materials [21, 22]. It has been observed that the critical velocity for the transition from stick–slip to smooth sliding is closely related to the property of the friction material surfaces, such as roughness and contact stiffness of the friction material surface. Further, the high surface stiffness has been found to increase the critical velocity for smooth sliding, suggesting the higher propensity of friction instability in a wider range of sliding velocities. Smooth friction material surfaces with glazed patches have been also observed to produce friction oscillations with larger amplitudes, which is consistent with the results shown by Eriksson et al. [5]. High propensity of squeal noise from the friction materials with smooth surfaces was also reported by Sherif [6]. He proposed a squeal index ($\gamma = \sqrt{\sigma/\beta}$) using two topographic parameters from sliding surfaces; the mean radius of asperities (β) and the standard deviation of the height distribution (σ), to derive a quantitative expression for noise propensity. He suggested that the high squeal index could reduce the propensity of squeal noise and the contact stiffness of the squealing pad/disk assembly was higher than that of a silent pad/disk assembly. The squeal index suggested by Sherif [6] was calculated using the topographic information from the friction material and disk surfaces listed in Table 3. The calculated squeal indices, which represent a high propensity of noise occurrence for lower values, were 0.23 (ZR 100), 0.16 (ZR 50), and 0.11 (ZR 3), indicating high noise occurrence when fine zircon is used.

In order to find the correlation between the friction instability observed in Figs. 7, 8, 9 and the surface properties, the surface topography and contact stiffness of the friction material specimens, which were altered by the size

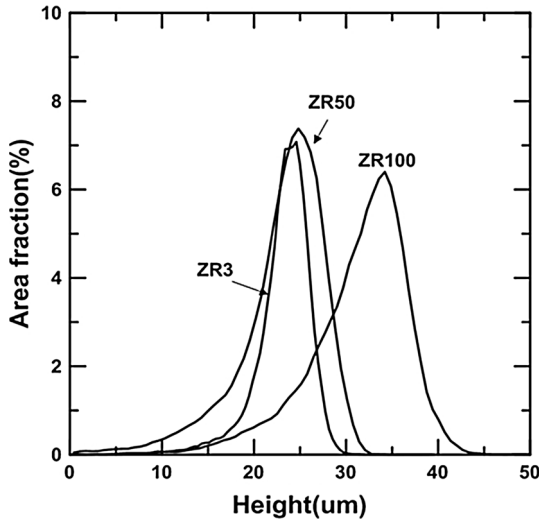

Fig. 10 The surface height distribution of the burnished surfaces measured using a laser confocal microscope. The width of the height distribution was smaller when smaller zircon particles were used in the friction material, indicating a smooth surface

of the zircon particles, were compared. Figure 10 shows the surface height distribution of the friction materials containing ZR 3, ZR 50, and ZR 100 after burnishing. The plot shows broader height distributions when coarser zircon particles were used, indicating that the entrenchment of the zircon particles into the friction layer differs because of differences in the sizes of the zircon particles, as shown in the micrographs in Fig. 5. The standard deviation of the surface height distribution in Table 3 supports the formation of a uniform surface in the case of the friction material containing fine zircon.

The contact stiffness of the friction material was also measured to find its effects on the friction instability during braking. Figure 11 shows the contact stiffness of the

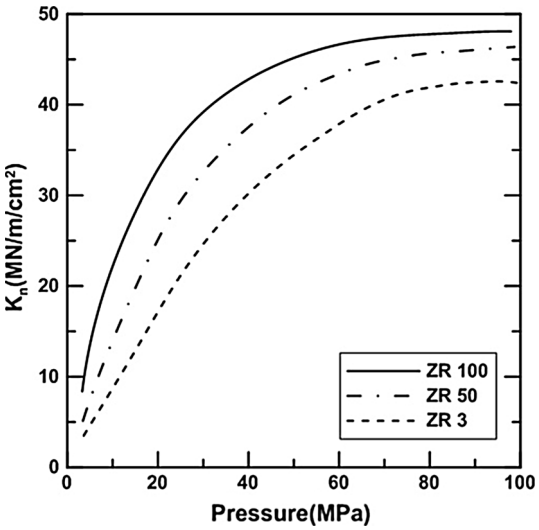

Fig. 11 Contact stiffness as a function of applied pressure

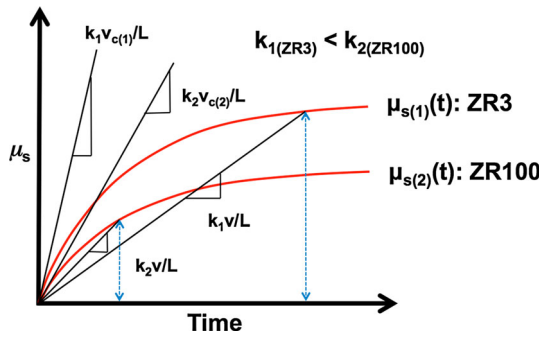

Fig. 12 A schematic illustrating the increase in the stick–slip amplitudes produced by the static coefficient of friction as a function of dwell time. k_1 and k_2 indicate the surface stiffness of the friction materials with fine (ZR 3) and coarse (ZR 100) zircon particles, respectively

friction material measured as a function of the applied pressure, which was obtained from the slope of the load–displacement plots. The contact stiffness (k_n) in the figure is composed of the surface stiffness (k_s) and the matrix stiffness (k_m), which are related by $k_n = (k_s \cdot k_m)/(k_s + k_m)$ [23]. The figure indicates that both the surface stiffness and the matrix stiffness are higher when coarse zircon particles are used. The high stiffness of the rough surface with better friction instability found in this study is contrary to the results shown by Lee et al. [24]. They measured the surface stiffness of the same friction material with different surface roughness levels and observed a higher stiffness in the case of smooth friction material surfaces and suggested a possible correlation between the friction instability and the surface roughness. High propensity of squeal noise from the friction material with smooth high stiffness surfaces was also reported by Sherif [6]. However, our results indicate that both contact stiffness and surface roughness has to be considered to find the correlation of the surface property and the friction instability.

The schematic in Fig. 12 explains the contribution from surface stiffness and roughness on the amplitude of friction oscillation during sliding. The figure shows the stick–slip amplitude determined by the level of the static coefficient of friction (μ_s), which is known to increase as a function of the dwell time [17]. This is based on the fact that $\mu_s(t)$ can be changed by surface roughness [17]. The figure indicates that $\mu_s(t)$ obtained from the smooth surface with ZR 3 is higher than the rough surface with ZR 100. The higher friction level of the friction material with ZR 3 in Fig. 3 and its smooth surface support the faster increase of μ_s as a function of dwell time.

The diagram also indicated that the stick–slip amplitude (height of the vertical arrows) can be decreased when the surface stiffness is higher. It shows that the amplitude from ZR 3 is greater than ZR 100 although the contact stiffness (k_2) from ZR 100 is greater than the contact stiffness (k_1) from ZR 3 due to the higher $\mu_s(t)$ level from the friction material with ZR 3. The larger amplitude of friction material with ZR3 observed in Fig. 7 at the same sliding velocity is, therefore, mainly attributed to the high $\mu_s(t)$ level. The lower critical velocity for smooth sliding in the case of the friction material with ZR 100 in Fig. 9 also can be explained from the schematic. This is because the critical velocity $v_{c(1)}$ for the friction material with ZR 3 is higher than $v_{c(2)}$ for the friction material with ZR 100 since k_1 is smaller than k_2 as shown in Fig. 12, and the slope of the initial tangent drawn to the $\mu_s(t)$ curve is equivalent to $k_i v_c/L$.

The interpretation based on the schematic in Fig. 12 suggests that the stick–slip amplitude and friction instability of a sliding couple can be affected by contact stiffness and roughness of the sliding surfaces. In particular, the change of the $\mu_s(t)$ level as a function of dwell time is found to be important to determine the friction instability along with contact stiffness. However, the precise determination of $\mu_s(t)$ as a function of the dwell time and the root causes for the change of $\mu_s(t)$ have not been confirmed using the friction material specimens in this study. However, this information appears to be very important to understand the triggering mechanism of the friction instability during sliding and the precise measurement of $\mu_s(t)$ is in progress considering the properties of microscopic asperity contacts on the sliding surface and environmental effects [25].

4 Conclusions

To understand the causes of brake noise and vibration, the friction oscillation of brake friction materials containing

zircon particles of three different sizes was studied using a reduced scale dynamometer. The size of the zircon particles strongly affected the friction level, roughness of the sliding surfaces, and the amplitude of the friction oscillation. The friction material specimen with fine zircon particles exhibited higher friction level and low contact stiffness with excessive friction material wear. The friction instability was also pronounced with the fine zircon becoming entrenched into the uniform surface. The critical velocity for smooth sliding increased when the zircon size is small, indicating a wider velocity span showing a high propensity of friction instability. The strong influence of the abrasive size on the friction instability indicates that the particle size strongly affects stiffness and roughness of the sliding surface and the possibility to control friction-induced noise and vibration by selecting abrasives with appropriate particle sizes.

Acknowledgments This study was supported by the Ministry of Knowledge Economy (MKE) through the Parts and Materials Development Program (No. 10040819).

References

1. Chen, F., Tan, C.A., Quaglia, R.L.: Disc Brake Squeal. SAE International, Warrendale (2006)
2. Duffour, P.: Noise Generation in Vehicle Brakes. Ph.D. thesis, Cambridge University (2002)
3. Crolla, D.A., Lang, A.M.: Brake Noise and Vibration—The State of the Art, pp. 165–174. Vehicle Tribology, Tribology Series (1991)
4. Lang, A.M.: An Investigation into Heavy Vehicle Drum Brake Squeal. Ph.D Thesis, Loughborough University (1994)
5. Eriksson, M., Bergman, F., Jacobson, S.: On the nature of tribological contact in automotive brakes. Wear **252**, 26–36 (2002)
6. Sherif, H.A.: Investigation on effect of surface topography of pad/disc assembly on squeal generation. Wear **257**, 687–695 (2004)
7. Lee, S.M., Shin, M.W., Lee, W.K., Jang, H.: The correlation between contact stiffness and stick–slip of brake friction materials. Wear **302**, 1414–1420 (2013)
8. Jang, H., Kim, S.J.: Brake friction materials. In: Sinha, S.K., Briscoe, B.J. (eds.) Polymer Tribology, pp. 506–532. Imperial College, London (2009)
9. Cho, M.H., Kim, S.J., Basch, R.H., Fash, J.W., Jang, H.: Tribological study of gray cast iron with automotive brake linings: the effect of rotor microstructure. Tribol. Int. **36**, 537–545 (2003)
10. Nicholson, G.: Facts About Friction. Gedoran America, Winchester (1995)
11. Cho, K.H., Jang, H., Hong, Y.S., Kim, S.J., Basch, R.H., Fash, J.W.: The size effect of zircon particles on the friction characteristics of brake lining materials. Wear **264**, 291–297 (2008)
12. Kim, S.S., Hwang, H.J., Shin, M.W., Jang, H.: Friction and vibration of automotive brake pads containing different abrasive particles. Wear **271**, 1194–1202 (2011)
13. Jang, H., Kim, S.J.: The effects of antimony trisulfide (Sb_2S_3) and zirconium silicate ($ZrSiO_4$) in the automotive brake friction materials on friction characteristics. Wear **239**, 229–236 (2000)
14. Lee, E.J., Hwang, H.J., Lee, W.G., Cho, K.H., Jang, H.: Morphology and toughness of abrasive particles and their effects on the friction and wear of friction materials: a case study with zircon and quartz. Tribol. Lett. **37**, 637–644 (2010)
15. Ma, Y., Martynková, G.S., Valášková, M., Matějka, V., Lu, Y.: Effects of $ZrSiO_4$ in non-metallic brake friction materials on friction performance. Tribol. Int. **41**, 166–167 (2008)
16. Matějka, V., Lu, Y., Jiao, L., Huang, L.: Simha Martynková, G., Tomášek, V.: Effects of silicon carbide particle sizes on friction-wear properties of friction composites designed for car brake lining applications. Tribol. Int. **43**, 144–151 (2010)
17. Rabinowicz, E.: The intrinsic variables affecting the stick-slip process. Proc. Phys. Soc. **71**(4), 668–675 (1958)
18. Gao, C., Kuhlmann-Willsdorf, D., Makel, D.D.: The dynamic analysis of stick–slip motion. Wear **173**, 1–12 (1994)
19. Persson, B.N.J.: Sliding friction: Physical Principles and Applications. Springer, Berlin (2000)
20. Fuadi, Z., Maegawa, S., Nakano, K., Adachi, K.: Map of low-frequency stick–slip of a creep groan. Proc. Inst. Mech. Eng. Part J: J. Eng. Tribol. **224**, 1235–1246 (2010)
21. Kim, S.H., Jang, H.: Friction and vibration of brake friction materials reinforced with chopped glass fibers. Tribol. Lett. **52**, 341–349 (2013)
22. Park, C.W., Shin, M.W., Jang, H.: Friction-induced stick–slip intensified by corrosion of gray iron brake disc. Wear **309**, 89–95 (2014)
23. Nishizawa, Y., Kosaka, K., Kurita, Y., Oura, Y.: Influence of pad thickness and surface roughness on pad stiffness. SAE paper 2012-01-1817 (2012)
24. Lee, S.M., Shin, M.W., Jang, H.: Friction-induced intermittent motion affected by surface roughness of brake friction materials. Wear **308**, 29–34 (2013)
25. Lee, W.K., Jang, H.: Moisture effect on velocity dependence of sliding friction in brake friction materials. Wear **306**, 17–21 (2013)